1 **For *Global and Planetary Change***

2 Co-variation of crenarchaeol and branched GDGTs in globally-distributed 3 marine and freshwater sedimentary archives

4 Susanne Fietz[*a], Carme Huguet[a], James Bendle[b], Marina Escala[a,1], Christopher
5 Gallacher[b], Lydie Herfort[c,2], Robert Jamieson[b], Alfredo Martínez-Garcia[a,3], Erin L.
6 McClymont[d,4], Vicky L. Peck[e], Fredrick G. Prahl[f], Sergio Rossi[a], Gemma Rueda[a], Anna
7 Sanson-Barrera[a], Antoni Rosell-Melé[a,g]

8 [a]ICTA, Universitat Autònoma de Barcelona, 08193 Cerdanyola del Vallès, Spain
9 [b]Glasgow Molecular Organic Geochemistry Laboratory, University of Glasgow, Glasgow, G12 8QQ,
10 UK.
11 [c]Department of Marine Organic Biogeochemistry, Royal Netherlands Institute for Sea Research (NIOZ),
12 1790, Den Burg, The Netherlands.
13 [d]School of Geography, Politics & Sociology, Newcastle University, Newcastle upon Tyne, NE1 7RU, UK
14 [e]British Antarctic Survey, Cambridge, CB3 0ET, UK
15 [f]College of Oceanic & Atmospheric Sciences, Oregon State University, Corvallis, OR 97331-5503, USA
16 [g]ICREA, Passeig Lluís Companys, 08010 Barcelona, Catalonia, Spain
17 [1]present address: Institute of Natural Resource Sciences, Zurich University of Applied Sciences,
18 Switzerland
19 [2]present address: Center for Coastal Margin Observation & Prediction, Oregon Health and Science
20 University, Portland, Oregon, USA
21 [3]present address: Eidgenössische Technische Hochschule (ETH) Zürich, Switzerland
22 [4]present address: Department of Geography, Durham University, Durham DH1 3LE, UK.
23 [*]Corresponding author: Susanne Fietz, Institut de Ciència i Tecnologia Ambientals (ICTA), Universitat
24 Autònoma de Barcelona (UAB), Campus UAB, 08193 Cerdanyola del Vallès, Catalonia, Spain, Tel.: +34
25 93 581 4219, Fax: +34 93 581 3331, email: susanne.fietz@uab.cat, alternative email: s_fietz@web.de

26 e-mail-adress of the co-authors:
27 Carme Huguet: Carme.Huguet@uab.cat
28 James Bendle: james.bendle@ges.gla.ac.uk
29 Marina Escala: marina.escala@zhaw.ch
30 Christopher.gallacher: Christopher.gallacher@glasgow.ac.uk
31 Lydie Herfort: herfortl@ebs.ogi.edu
32 Alfredo Martínez-Garcia: alfredo.martinez-garcia@erdw.ethz.ch
33 Erin McClymont: erin.mcclymont@durham.ac.uk
34 Vicky Peck: vlp@bas.ac.uk
35 Fred Prahl: fprahl@coas.oregonstate.edu
36 Sergio Rossi: Sergio.Rossi@uab.cat
37 Gemma Rueda: gemma.rueda@uab.cat
38 Anna Sanson-Barrera: Anna.Barrera@uab.cat
39 Antoni Rosell-Melé: antoni.rosell@uab.cat
40

ABSTRACT

Two major types of glycerol dialkyl glycerol tetraethers (GDGTs) are commonly used in paleoecological and paleoclimatological reconstructions: isoprenoidal and branched GDGTs. In aquatic environments it was originally assumed that isoprenoidal GDGTs, especially crenarchaeol, derive mainly from aquatic Thaumarchaeota, whilst branched GDGTs are an allochthonous input derived from soil Bacteria. Recently, direct co-variation of crenarchaeol and branched GDGTs has been described in two marine sedimentary records, and this observation suggests *in situ* production of branched GDGTs is possible at least in some aquatic environments. After investigating 30 published and unpublished data sets from downcore and surface sediments as well as sediment traps from 15 distinct regions around the world we found a widespread significant correlation between concentrations of branched GDGTs and crenarchaeol ($p<0.01$; $r^2=0.57$-0.99), even when normalized against TOC, where available. These data sets include freshwater and marine environments with varying distances from the shore, varying redox conditions and different terrestrial matter input pathways. Our findings from this large-scale data set suggest that a common or mixed source for both GDGT types is actually commonplace in lacustrine and marine settings.

Keywords: Archaea; branched GDGTs; crenarchaeol; in situ production; isoprenoid GDGTs; lakes; oceans

1. INTRODUCTION

The glycerol dialkyl glycerol tetraethers (GDGTs) are cell membrane lipids of Archaea and Bacteria that are used in paleolimnology and paleoceanography to track changes in archaeal abundance, terrestrial organic matter input into aquatic systems and to estimate past water and air temperatures. The two major types of GDGTs currently used have isoprenoidal and branched structures.

Mesophilic Archaea synthesize isoprenoidal GDGTs and the isoprenoidal GDGT crenarchaeol, for example, has become a marker for Thaumarchaeota (Sinninghe Damsté et al., 2002). Thaumarchaeota, formerly known as Crenarchaeota group I (Brochier-Armanet et al., 2008), are ubiquitously distributed in marine environments (Fuhrman et al., 1992; DeLong et al., 1998; Massana et al., 2000) as well as in lakes (Schleper et al., 1997; Keough et al., 2003; Casamayor and Borrego, 2009). Consequently, isoprenoidal GDGTs and especially crenarchaeol, have been found globally in marine and lacustrine water column and sediment samples (Powers et al., 2010; Kim et al., 2010).

The branched GDGTs have been predominantly found in terrestrial settings such as peat bogs and soils (Weijers et al., 2006a), but also in sedimentary settings receiving significant terrestrial input (Hopmans et al., 2004). The glycerol stereochemistry of the branched GDGTs supports a bacterial provenance (Weijers et al., 2006b) and recently a branched GDGT could be identified in two cultures of Acidobacteria (Sinninghe Damsté et al., 2011). However, these Bacteria are aerobes and the highest branched GDGT concentrations are found in low-oxygen environments, suggesting that the branched GDGTs are likely synthesized by other groups of Bacteria as well (Sinninghe-Damsté et al., 2011).

Three main indices have been proposed for paleo-reconstructions in marine and lacustrine sedimentary records using isoprenoidal and branched GDGTs, which are the TEX_{86} (Schouten et al., 2002), the MBT/CBT (Weijers et al., 2007) and the BIT (Hopmans et al., 2004). The basic premise for those indices is that isoprenoidal GDGTs are of aquatic origin and that the branched GDGTs are exclusively terrestrially-derived and transported to the aquatic environment through erosion, rivers, ice rafting, etc. However, isoprenoidal GDGTs including crenarchaeol have also been found in terrestrial environments, e.g., in peat bogs and soils (Gattinger et al., 2003; Leininger et al., 2006; Weijers et al., 2006a). Furthermore, a mixed allochthonous and autochthonous source for branched GDGTs has been recently suggested in lakes (Sinninghe Damsté et al., 2009; Bechtel et al., 2010; Blaga et al., 2010; Tierney et al., 2010; Zink et al., 2010; Sun et al., 2011). Peterse et al. (2009) and Zhu et al. (2011) also proposed an autochthonous source for branched GDGTs in marine coastal sites. In contrast, Yamamoto et al. (2008) suggested an allochthonous source for crenarchaeol in the central Arctic Ocean. Yamamoto et al. (2008) and Zhu et al. (2011) based their conclusions on the strong correlation they observed between branched GDGT and crenarchaeol concentrations.

In the present study, we show the pervasive significant correlation between branched GDGTs and crenarchaeol in a wide range of aquatic environments. These include sediment trap samples, surface sediments and downcore records from lacustrine and marine settings. The sites were not initially selected for the purpose discussed here and several data sets used for this large-scale comparative study have already been published (Herfort et al., 2006; Huguet et al., 2007, 2011; Bendle et al., 2010; Fietz et al., 2011a, 2011b). We discuss the possible mechanisms responsible for such a global

pattern, including the prospect that branched GDGTs have a significant autochthonous source in some aquatic settings.

2. REGIONAL SETTINGS

The map in Figure 1 identifies the sites included in this paper and further information on each sampling location is provided in Table 1. We show sediment trap, surface sediment and downcore data from lakes in Russia, France, and Turkey, as well as data for water column (filtered particulate matter), sediment trap, and surface and downcore sediment samples from locations in the Atlantic, Pacific, North Sea, and Mediterranean. Brief descriptions of all locations and data sets are given in Appendix 1.

3. MATERIAL AND METHODS

Sample processing methods are diverse as the data were obtained by different research groups with a focus initially outside the scope of the present analysis. All methods are briefly described, including those concerning already published data sets (Herfort et al., 2006; Huguet et al., 2007, 2011; Escala 2009; Bendle et al., 2010; Fietz et al., 2011a, 2011b; McClymont et al., in press) so that they can be compared. The numbering given for extraction, fractionation and analyses refer to the respective data sets listed in Table 1.

3.1. Lipid extraction

All samples were freeze-dried and sediments homogenized. Solvents used for extraction were mixtures of dichloromethane and methanol (DCM/MeOH). **E1**) Microwave assisted extraction (as in Huguet et al., 2007, 2011; Escala et al. 2009; Fietz et al.

2011a, 2011b; McClymont et al., in press), **E2**) Accelerated Solvent Extractor (ASE 200, Dionex; as in Herfort et al., 2006), **E3)** Ultrasonic extraction (as in Schouten et al., 2007), **E4)** 24h Soxhlet extraction (as in Bendle et al., 2010).

3.2. Fractionation, purification

F1) Extracts were analyzed without further fractionation (as in Fietz et al., 2011a). **F2**) Extracts were fractionated with preparative column chromatography using activated alumina and sequential eluent mixtures of hexane (HEX)/DCM, HEX/DCM and DCM/MeOH (as in Huguet et al., 2011). **F3**) Extracts were fractionated with preparative column chromatography using activated or deactivated silica (1 or 5% H_20) and sequential eluents HEX, DCM or a mixture of HEX/DCM and DCM/MeOH (as in Herfort et al., 2006). **F4**) Extracts were redissolved in HEX/DCM and injected in a Thermo Surveyor HPLC system equipped with a Lichrosphere silica column. Fractionation was achieved running sequentially HEX, DCM, and acetone (as in Fietz et al. 2011a). **F5**) Extracts were hydrolyzed overnight with 8% potassium hydroxide (KOH) in MeOH. The GDGT-containing fraction was recovered with hexane (as in Escala, 2009). **F6)** Extracts were redissolved in chloroform and eluted through 500 mg aminopropyl mini-columns running sequentially chloroform/2-propanol and diethyl ether/acetic acid (as in Ruiz et al., 2004).

3.3. Analysis

All polar fractions were redissolved in HEX/n-propanol or HEX/isopropanol prior to injection into the respective HPLC-MS system. All instruments used in this study were equipped with an atmospheric pressure chemical ionization (APCI) source. Mixtures of HEX/n-propanol or HEX/isopropanol were used as eluents either in gradient or isocratic modes. **A1**) A Dionex P680 HPLC system coupled to a Thermo Finnigan TSQ

157 Quantum Discovery Max quadrupole mass spectrometer (MS) was used with a Tracer
158 Excel CN column (as in Fietz et al., 2011a, 2011b. **A2**) An Agilent 1100 HPLC system
159 coupled to a Bruker Esquire 3000 ion trap MS was used and a Nucleosil CN column (as
160 in Escala, 2009). **A3)** An HP 1100 Series HPLC-MS system was used and a Prevail
161 Cyano column (Herfort et al., 2006; Huguet et al., 2007). A3 analyses were done in
162 triplicate and averages are presented in this study. **A4)** An Agilent 1100 series/HP 1100
163 MSD series HPLC-MS system was used and an Alltech Prevail Cyano column (Bendle
164 et al., 2010). **A5**) A Thermo Finnigan LCQ MS was used with a Grace Prevail Cyano
165 column (McClymont et al., in press). GDGTs in all **A1-A5** analyses were monitored in
166 selected ion monitoring (SIM) mode at *m/z* 1302, 1300, 1298, 1296, 1292 (isoprenoidal
167 GDGTs, with 1292 referred here as crenarchaeol), 1050, 1036, and 1022 (major
168 branched GDGTs), and *m/z* 1048, 1046, 1034, 1032, 1020, and 1018 (minor, cyclized
169 branched GDGTs).

170 **3.4. Normalization**

171 Since we can not rule out artefacts in concentrations derived from the different
172 instrument and quantification methods used across the various laboratories included in
173 this study, all data were normalized and data are given here as relative units.
174 Normalization was accomplished by finding the sample with the highest crenarchaeol
175 relative unit in a given data set and then dividing all crenarchaeol and branched GDGT
176 data in that set to this reference value.

177 **3.5. TOC and chlorophyll**

178 For some sample sets, reference data for total organic carbon (TOC) and chlorophyll *a*
179 transformation products (including all pheopigments) were available, partly from
180 published studies (Herfort et al., 2006; Fietz et al., 2007, 2011a; Huguet et al., 2007,

2011; Martínez-Garcia et al., 2009). This information allows the data to be expressed per gram TOC or per gram chlorophyll degradation products. For the Lake Baikal interglacial record, TOC and chlorophyll transformation products analyses were carried out on parallel samples (same core) to the above described GDGT analyses within an earlier study (Fietz et al., 2007). TOC analyses for the Drammensfjord were carried out on parallel samples to the above described GDGT analyses as described by Huguet et al. (2007). Chlorophyll transformation products for sediment trap samples from Lake Van (Huguet et al., 2011) and Lake Baikal, as well as downcore samples from Fram Strait (Fietz et al., 2011a), subantarctic Atlantic (Martínez-Garcia et al., 2009), and Guaymas Basin were measured on the total lipid extracts before further fractionation was carried out for GDGT analyses. The method is described by Martínez-Garcia et al. (2009).

4. RESULTS

In almost all sample sets, the abundance of crenarchaeol is significantly ($p<0.001$) correlated to the combined abundance of the major branched GDGTs (Figures 2 and 3, Table 1), as well as to the combined abundance of the minor cyclized branched GDGTs, (Table 1). This strong correlation is observed in samples from freshwater and marine environments at varying distances from the shore, over a range of redox conditions and with different pathways of terrestrial matter input. No significant correlation between crenarchaeol and branched GDGTs was found in only three out of the 30 data sets examined in this study.

4.1. Data sets with significant correlations between crenarchaeol and branched GDGTs

4.1.1. Lakes

205 Significant correlations ($p < 0.01$) are found in down core sediment sample sets from
206 Lake Baikal, Lake Bourget, and Lake Van even though different interglacial and glacial
207 cycles are considered, as well as in surface sediments and sediment trap material (Fig.
208 2). All correlations have coefficients of determination (r^2) higher than 0.8 and a wide
209 range of slope values (Table 1). Variation in slope values is indicative of the relative
210 concentration change between branched GDGTs and crenarchaeol. It must be noted that
211 in an intercalibration study (Schouten et al., 2009) the BIT index, which resembles the
212 slope of branched GDGTs versus crenarchaeol, varied greatly between individual LC-
213 MS systems (e.g., BIT values ranging from 0.25 to 0.82 on a scale from 0 to 1).
214 However, in the present study a wide range of slope values is also found for sample sets
215 measured on the same LC-MS (e.g., 0.4 to 4.1 for LC-MS system A1, see Table 1) and
216 the coefficient of variation (CV, calculated as standard deviation per mean value) is
217 higher for the lake slope values (CV=0.5) than for the BIT in the intercalibration study
218 (CV=0.2). Significant correlations are furthermore observed between cyclized branched
219 GDGTs and crenarchaeol in the lakes and the r^2-values are only slightly lower than
220 those calculated for the major branched GDGT versus crenarchaeol correlations (Table
221 1).

222 *4.1.2. Marine Settings*

223 Significant correlations ($p < 0.01$) between the major brGDGTs and crenarchaeol are
224 observed in most downcore records of our marine sites (Fig. 3A-J), although the
225 environmental conditions as well as pathways and amounts of terrestrial matter input
226 strongly differ between the studied sites. All r^2 values are higher than 0.57 (Table 1).
227 Such strong correlation is not only found through time at certain sites, but also in two
228 surface sediment compilations of the North and Catalan Seas (Table 1, Figs. 3K,L). As
229 for lakes, slopes vary over a wide range (0.01 to 0.9; Table 1). Some sites that receive

more allochthonous material through eolian input (Guaymas Basin, equatorial Pacific, subantarctic Atlantic) than by river discharge have shallow slopes (≤0.07). The equatorial Atlantic site, however, which predominantly receives dust input from the Sahara, has a remarkably steep slope of 0.61 (even though measured on the same LC-MS than the subantarctic Atlantic samples that have a slope of 0.06, see Table 1). Significant correlations are also observed between cyclized branched GDGTs and crenarchaeol in the marine sites and again (as for lakes) the r^2 values are in a similar range as those calculated for the major branched GDGT versus crenarchaeol correlations (Table 1).

4.2. Sites without significant correlation between crenarchaeol and major branched GDGTs

No significant correlation is found in two downcore records and one water column sample set (Fig. 4). Lake Yamozero is, at present, a shallow lake with large lake level variations, which have caused major hiatuses in the record (Henriksen et al., 2008). This may explain the large scatter in the branched GDGTs vs. crenarchaeol correlation. The NE Atlantic site lies within the impact zone of the British Ice Sheet and the record is characterized by the sudden input of abundant and very ancient terrestrial organic matter (Peck et al., 2006), which might have caused the scatter. Lack of significant correlation is also observed in the water samples from Chipana, off Chile. One sample deviated from the five others and this outlier (February 2007 surface sample) was mainly due to low crenarchaeol concentration instead of exceptionally high branched GDGT concentrations (Fig. 4).

4.3. Correlation for data sets normalized to total organic carbon or chlorophyll transformation products

When possible, the GDGT data were normalized to TOC in order to assess the possible impact of organic matter diagenesis on the correlation (Fig. 5). Where TOC data are available, the brGDGTs/TOC vs. crenarchaeol/TOC correlations are still significant at $p<0.01$ (Baikal Interglacial, Buguldeyka Uplift, Drammensfjord and North Sea; Fig. 5; Table 2). Yamamoto et al. (2008) and Zhu et al. (2011) both also published significant correlations between TOC normalized branched GDGTs and crenarchaeol. Only in one data set (Lake Van) the relationship between brGDGTs/TOC and crenarchaeol/TOC is deteriorated ($p=0.05$; Fig. 5, Table 2).

For many records, TOC data are not available. Chlorophyll *a* transformation products (including phaeopigments) are considered instead, because they track the aquatic primary productivity component of the deposited organic matter (Harris et al., 1996). Chlorophyll *a* produced in the water column is strongly degraded before final burial and hence, normalization to chlorophyll transformation products (Chl.) reduces the impact of diagenesis in the data sets similarly to TOC. The fit of brGDGTs/Chl. versus crenarchaeol/Chl. is still significant ($p<0.01$) for Lake Baikal and Lake Van seasonal traps, as well as for Lake Baikal Interglacial, Guaymas Basin, Fram Strait, and subantarctic Atlantic records ($r^2 = 0.58$-0.99; Table 2).

5. DISCUSSION

Crenarchaeol is considered a marker for mesophilic Thaumarchaeota of predominantly aquatic origin (Sinninghe Damsté et al., 2002), while branched GDGTs are proposed markers for soil Bacteria (Weijers et al., 2010). Positive correlation between branched GDGTs and crenarchaeol was reported previously for the Central Arctic (Yamamoto et al., 2008) and the East China Sea shelf (Zhu et al., 2011). Since we observe it in all, but

three, of the 30 data sets examined here, this phenomenon is a global feature. The key question to answer is: how can two markers from purportedly two different source environments display such strong correlation in so many different settings?

5.1. Amplification of correlation by diagenesis

Preservational efficiency is an important factor to explain variability in downcore sedimentary signals (Furlong and Carpenter, 1988; Calvert and Pedersen, 1992). Earlier studies demonstrated that oxygen exposure can cause a decrease in GDGT concentration by one or two orders of magnitude (Schouten et al., 2004; Zonneveld et al., 2010). Amplification in the dry weight related concentrations due to the settling and preservation conditions can therefore not be excluded as an explanation for the observed correlations in the sedimentary data sets. However, if diagenetic factors primarily control the biomarker concentrations, the significant correlation between brGDGTs and crenarchaeol normalized to dry weight should be largely deteriorated when both are normalized to TOC. GDGTs are associated to their respective organic matter sources. Input, settling and preservation of GDGTs are therefore closely related to the TOC, which contains aquatic and terrestrial compounds. TOC-normalization of the GDGTs therefore minimizes temporal or regional variability in the amount of organic matter deposited and/or changes in preservation conditions for given data sets. However, in two Lake Baikal records, the Drammensfjord record and the North Sea surface sediment compilation, the correlations between brGDGTs/TOC and crenarchaeol/TOC are diminished but remain significant (Fig. 5, Table 2). brGDGTs/TOC and crenarchaeol/TOC are also correlated in sample sets from the Central Arctic (Yamamoto et al., 2008) and China Sea (Zhu et al., 2011). The regression is deteriorated at insignificant level in only one data set (Lake Van). If plotted against chlorophyll degradations products (chl.), which are also affected by the preservational conditions,

303 the correlations of brGDGTs/chl. versus crenarchaeol/chl. are also still significant
304 (Table 2).

305 Furthermore, diagenesis differs between branched and isoprenoid GDGTs. Huguet et
306 al. (2008) found that over long time spans (>100 ky) branched GDGTs are better
307 preserved than isoprenoidal GDGTs. At sites or time spans with lower overall
308 productivity and sedimentation, and therefore prevailing oxic conditions, the
309 brGDGTs/crenarchaeol ratio might thus be biased towards higher values. Such redox
310 condition dependant shift in the brGDGTs/crenarchaeol ratio should have reduced the
311 correlation. Therefore, diagenetic processes are probably not the primary driving factors
312 for the observed correlations.

313 **5.2. Correlations triggered by physical processes in different source**
314 **environments**

315 Very few environmental factors might have a direct and equal influence to both
316 aquatic Thaumarchaeota and GDGT-producing soil Bacteria. Temperature, for example,
317 which would be a global feature for soil and aquatic systems, has only been shown to be
318 of major influence for the relative distribution of isoprenoid GDGT distributions but not
319 for absolute abundances (Schouten et al., 2002). pH and anaerobic conditions have been
320 proposed as major environmental factors driving the concentration of branched GDGTs
321 in soils (Weijers et al., 2007), but there is no published study about what environmental
322 factor drives the crenarchaeol concentration in the aquatic settings.

323 The observed co-variations between crenarchaeol and branched GDGTs might instead
324 result to some extent from parallel or sequential effects. For example, if branched
325 GDGTs indicate allochthonous matter input, they would be coupled to nutrient input
326 which may result in site fertilization. A likely scenario to explain the co-variation

between branched GDGTs and crenarchaeol might therefore be that increases in branched GDGTs would be an indicator of e.g., erosion, dust, or ice-rafted debris input. This might serve as a substrate for the Thaumarchaeota or contain nutrients that fertilize the system and induce increased deposition. However, it remains questionable if fertilization can possibly explain the worldwide observed correlations, including sites unlikely to be resource limited (e.g. Lake Baikal, Lake Bourget, Lake Van, North Sea).

5.3. Correlations due to common source environment of both GDGT types

A common terrestrial origin has been suggested by Yamamoto et al. (2008) for crenarchaeol and branched GDGTs in central Arctic sediments. Yamamoto et al. (2008) proposed that both types of GDGTs were introduced by terrestrial matter trapped in the ice and released as the ice drifted and melted over the central Arctic. However, a common terrestrial origin is an unlikely explanation for correlations observed globally. In contrast, Zhu et al. (2011) suggested a common aquatic source for crenarchaeol and branched GDGTs in the East China Sea. Co-variation of Thaumarchaeota and Bacteria has been shown in water column studies based on metagenomic surveys (Beman et al., 2011). Therefore, co-production of branched GDGTs in aquatic settings by Bacteria may account for the observed correlation.

From the distribution of branched GDGTs in soils (Weijers et al. 2007, 2010), it actually seems that they are produced by waterborne Bacteria as they seem to be found predominantly around the water table or in soil pore water. Furthermore, brGDGT-producing Bacteria have been proposed to be anaerobic (Weijers et al., 2006b). This suggests that they could possibly also be produced in the water column (oxygen minimum zone), at the sediment surface, or in anoxic interstitial spaces within the sediments. Aquatic *in situ* production of branched GDGTs has been in fact suggested in

many earlier studies, predominantly in lakes (Sinninghe Damsté et al., 2009; Bechtel et al., 2010; Blaga et al., 2010; Tierney et al., 2010; Zink et al., 2010; Sun et al., 2011), and also in two marine settings (Peterse et al., 2009; Zhu et al., 2011).

5.4. Mixed origins

Part of the branched GDGTs detected in lakes and oceans must be of terrestrial origin because in almost all aquatic settings there is evidently some terrestrial matter input through erosion, river run-off, or wind transport. Furthermore, branched GDGTs and crenarchaeol are not correlated if we pool all of the data into one global set, because of the large differences in regression slopes. Partly these differences might be attributed to the analytical constraints (Escala et al., 2009; Schouten et al., 2009). However, the slopes varied over wide ranges even if analyzed with the same LC-MS (e.g., 0.06 and 0.6 for subantarctic Atlantic and equatorial Atlantic). Furthermore, the coefficient of variation of our slope values is much higher (0.88) than for the BIT values in the Schouten et al. (2009) intercalibration study (0.24), indicating that the slope values range is beyond the LC-MS-based differences. Most slopes are higher in the lakes than in the marine sites (Table 1). This could support the original premise that crenarchaeol is autochthonous and branched GDGTs are allochthonous or indicate a higher *in situ* production of branched GDGTs in lakes than in oceans or a combination of both. It is therefore most likely that both GDGTs types have a mixed autochthonous and allochthonous origin. This mixed origin has consequences for the use of GDGT derived proxies for paleoclimatic reconstructions, as the reliability of both BIT and MBT/CBT indices depends on the assumption that the branched GDGTs deposited in the sediments are exclusively of terrestrial origin.

6. CONCLUSION

Until recently, it has been widely accepted that in sedimentary archives crenarchaeol is predominantly derived from aquatic Archaea and branched GDGTs are derived from soil Bacteria. In this study, we show that branched GDGTs are correlated to crenarchaeol on a region by region basis in globally distributed records. Certainly, the correlation is partly due to an amplification effect caused by preservation of both GDGT types in sedimentary settings with high preservation potential, but diagenesis can not be the one and only process driving the observed tight correlations. Various scenarios of common physical driving factors or cascading effects are plausible to explain the correlations at specific sites. Those are, however, not satisfying to explain the global pattern. Globally considered, our findings of strong correlations coupled to a wide range of slopes indicate a more complex situation, suggesting that a mixed source for both GDGT types is commonplace in lacustrine and marine settings.

Acknowledgements: N. Moraleda is thanked for sample processing and analysis. The authors thank R. Gyllencreutz, R. Spielhagen, A. Prokopenko, J. Jacob for providing samples. The authors furthermore thank teams from CONTINENT, IMAGES IV, MONA, and ANTROMARE. J.B. thanks the staff and colleagues at the NERC Life Sciences Mass Spectrometry Facility (Bristol), the Organic Geochemistry Unit at University of Bristol, and the Department of Marine Organic Biogeochemistry at Royal Netherlands Institute for Sea Research (NIOZ).

S.F. thanks the Deutsche Forschungsgemeinschaft (DFG) for a Postdoctoral Fellowship (FI 1466/1-1). S.F. and C.H. thank the Spanish Ministerio de Ciencia e Innovación (MICINN) for Juan de la Cierva fellowships. M.E. thanks the Generalitat de Catalunya. J.B. thanks the Natural Environment Research Council (NE/C508934/1), the Ocean Drilling Programme (IODP), The Carnegie Trust for the Universities of Scotland, and the Projects 'Millennium' and IMAGES. E.L.M. thanks Natural Environment Research Council (NE/E00119X/1) and the IMAGES programme. A.M.G. and G.R. thank the MICINN (AP2004-7151 and AP2008-00801). F.P. acknowledges support from the National Science Foundation sponsored Center for Coastal Margin Observation and Prediction. S.R. was co-financed with Beatriu de Pinós (2006 BP-B1 00069) and Ramón y Cajal Contracts (RyC-2007-01327). A.R.M. acknowledges support from the European Commission Marie Curie-IOF (235626). Support for this work was furthermore provided by the MICINN as research funds (POL2006-02990, CGL2008-03288-E, CGL2010-15000).

REFERENCES

Bechtel, A., Smittenberg, R.H., Bernasconi, S.M., Schubert, C.J., 2010. Distribution of branched and isoprenoid tetraether lipids in an oligotrophic and a eutrophic Swiss lake: Insights into sources and GDGT-based proxies. Org. Geochem. 41, 822-832.

Beman, J.M., Steele, J.A., and Fuhrman J.A., 2011. Co-occurrence patterns for abundant marine archaeal and bacterial lineages in the deep chlorophyll maximum of coastal California. ISME J. 5, 1077–1085.

Bendle, J.A., Weijers, J.W.H., Maslin, M.A., Sinninghe, Damsté J.S., Schouten, S., Hopmans, E.C., Boot, C.S. and Pancost, R.D., 2010. Major changes in glacial and Holocene terrestrial temperatures and sources of organic carbon recorded in the Amazon fan by tetraether lipids. Geochem. Geophys. Geosyst. 11, Q12007, doi:10.1029/2010GC003308

Blaga, C.I., Reichart, G.-I., Schouten, S., Lotter, A.F. Werne, J.P., Kosten, S., Mazzeo , N., Lacerot, G., Sinninghe Damsté, S.J., 2010. Branched glycerol dialkyl glycerol tetraethers in lake sediments: Can they be used as temperature and pH proxies? Org. Geochem. 41, 1225-1234.

Brochier-Armanet, C., Boussau, B., Gribaldo, S., Forterre, P., 2008. Mesophilic Crenarchaeota: proposal for a third archaeal phylum, the Thaumarchaeota, Nat. Rev. Microbiol. 6, 245-52.

Calvert, S.E., Pedersen, T.F., 1992. Organic matter accumulation, remineralization and burial in an anoxic coastal sediment. In: Whelan, J.K., Farrington, J.W. (Eds.), Organic Matter: Productivity, Accumulation and Preservation in Recent and Ancient Sediments. Columbia Univ. Press, New York, pp. 231–263.

Casamayor, E.O., Borrego C.M., 2009. Archaea in inland waters. In: Likens G. (Ed.), Encyclopedia of Inland Waters. Academic Press, Elsevier UK, vol. 3, pp. 167-181.

DeLong, E.F., 1998. Everything in moderation: archaea as 'non-extremophiles'. Curr. Opin. Genet. Dev. 8, 649–654.

Escala, M., 2009. Application of tetraether membrane lipids as proxies for continental climate reconstruction in Iberian and Siberian lakes. Ph. D. thesis, Universitat Autònoma de Barcelona (http://www.tdx.cat/TDX-1020109-144857)

Escala, M., Fietz, S., Rueda, G., Rossell-Melé, A., 2009. Analytical considerations for the use of the paleothermometer Tetraether Index86 and the Branched vs Isoprenoid Tetraether Index regarding the choice of cleanup and instrumental conditions. Anal. Chem. 81, 2701–2707.

Fietz, S., Nicklisch, A., Oberhänsli, H., 2007. Phytoplankton response to climate changes in Lake Baikal during the Holocene and Kazantsevo Interglacials assessed from sedimentary pigments. J. Paleolimn. 37, 177-203.

Fietz, S., Martínez-Garcia, A., Rueda, G., Peck, V.L., Huguet, C., Escala, M., Rosell-Melé, A., 2011a. Crenarchaea and phytoplankton coupling: Common trigger or metabolic dependence? Limnol. Oceangr. 56, 1907-1916.

Fietz, S., Martínez-Garcia, A., Huguet, C., Rueda, G., Rosell-Melé, A., 2011b, Constraints in the application of the Branched and Isoprenoid Tetraether (BIT) index as a terrestrial input proxy, J. Geophys. Res. 116, C10032 doi:10.1029/2011JC007062.

Fuhrman, J.A., McCallum, K., Davis, A.A., 1992. Novel major archaebacterial group from marine plankton. Nature 356, 148–149.

Furlong, E.T., Carpenter, R., 1988. Pigment preservation and remineralization in oxic coastal marine sediments. Geochim. Cosmochim. Ac. 52, 87–99.

Gattinger, A., Günthner, A., Schloter, M., Munch, J.C., 2003. Characterisation of Archaea in soils by polar lipid analysis. Acta Biotechnol. 23, 21-28.

460 Harris, P.G., Zhao, M., Rosell-Melé, A., Tiedemann, R., Sarnthein, M., Maxwell, J.R.
461 1996. Chlorin accumulation rate as a proxy for Quaternary marine primary
462 productivity. Nature 383, 63–65.
463 Henriksen, M., Mangerud, J., Matiouchkov, A., Murray, A.S., Paus, A., Svendsen, J.I.
464 2008. Intriguing climatic shifts in a 90 kyr old lake record from northern Russia.
465 Boreas 37, 20–37.
466 Herfort, L., Schouten, S., Boon, J.P., Wolering, M., Baas, M., Weijers, J.M.H., and
467 Sinninghe Damsté, J.S., 2006. Characterization of transport and deposition of
468 terrestrial organic matter in the southern North Sea using the BIT index. Limnol.
469 Oceanogr. 51, 2196–2205.
470 Hopmans, E.C., Weijers, J.W.H., Schefuss, E., Herfort, L., Sinninghe Damsté, J.S.,
471 Schouten S., 2004. A novel proxy for terrestrial organic matter in sediments based on
472 branched and isoprenoid tetraether lipids. Earth Planet. Sc. Lett. 224, 107–116.
473 Huguet, C., Smittenberg, R.H., Boer, W., Sinninghe Damsté, J.S., and Schouten, S.
474 2007. Twentieth century proxy records of temperature and soil organic matter input
475 in the Drammensfjord, southern Norway. Org. Geochem. 38, 1838-1849.
476 Huguet, C., de Lange, G.J., Middelburg, J.J., Sinninghe Damsté, J.S., Schouten, S.
477 2008. Selective preservation of soil organic matter in oxidized marine sediments
478 (Madeira Abyssal Plain). Geochim. Cosmochim. Acta 72, 6061-6068.
479 Huguet , C., Fietz, S., Stockhecke, M., Sturm, M., Anselmetti, F.S., Rosell-Mele, A.
480 2011. Biomarker seasonality study in Lake Van, Turkey. Org. Geochem. 42, 1289-
481 1298.
482 Keough, B.P., Schmidt, T.M., Hicks, R.E., 2003. Archaeal nucleic acids in picoplankton
483 from great lakes on three continents. Microb. Ecol. 46, 238–248.
484 Kim, J.-H., Meer, J.v.d., Schouten, S., Helmke, P., Willmott, V., Sangiorgi, F., Koç, N.,
485 Hopmans, E.C., and Sinninghe Damsté, J.S., 2010. New indices and calibrations
486 derived from the distribution of crenarchaeol isoprenoid tetraether lipids:
487 implications for past sea surface temperature reconstructions. Geochim. Cosmochim.
488 Ac. 74, 4639–4654.
489 Leininger, S., Urich, T., Schloter, M., Schwark, L., Qi, J., Nicol, G.W., Prosser, J.I.
490 Schuster, S. C., Schleper, C., 2006. Archaea predominate among ammonia-oxidizing
491 prokaryotes in soils. Nature 442, 806-809.
492 Martínez-Garcia, A., Rosell-Melé, A., Geibert, W., Gersonde, R., Masqué, P., Gaspari,
493 V., Barbante, C., 2009. Links between iron supply, marine productivity, sea surface
494 temperatures and CO_2 over the last 1.1My. Paleoceanography, PA1207. DOI:
495 10.1029/2008PA001657
496 Massana, R, DeLong, E.F., Pedros-Alio, C., 2000. A few cosmopolitan phylotypes
497 dominate planktonic archaeal assemblages in widely different oceanic provinces.
498 Appl. Environ. Microbiol. 66, 1777–1787.
499 McClymont E.L., Ganeshram R., Pichevin L.E., Talbot H.M., van Dongen B.E.,
500 Thunell R.C., Haywood A.M., Singarayer J.S., Valdes P.J., *in press*. Sea-surface
501 temperature records of Termination 1 in the Gulf of California: challenges for
502 seasonal and inter-annual analogues of tropical Pacific climate change
503 (2011PA002226).
504 Peck, V. L., Hall, I., Zahn, R., Elderfield, H., Grousset, F., Hemming, S.R., Scourse,
505 J.D., 2006. High resolution evidence for linkages between NW European ice sheet
506 instability and Atlantic Meridional Overturning Circulation. Earth Planet. Sc. Lett.
507 243, 476-488.
508 Peterse, F., Kim, J.-H., Schouten, S., Klitgaard Kristensen, D., Koç, N., Sinninghe
509 Damsté, J.S., 2009. Constraints on the application of the MBT/CBT

paleothermometer at high latitude environments (Svalbard, Norway). Org. Geochem. 40, 692-699.
Powers, L.A., Werne, J.P., van der Woude, A.J., Sinninghe Damsté, J.S., Hopmans, E.C., and Schouten, S., 2010. Applicability and calibration of the TEX_{86} paleothermometer in lakes. Org. Geochem. 41, 404–413.
Ruiz, J., Antequera, T., Andres, A.I., Petron, M.J., Muriel, E., 2004. Improvement of a solid phase extraction method for analysis of lipid fractions in muscle foods. Anal. Chim. Acta 520, 201-205.
Schleper, C., Holben, W., Klenk, H.-P., 1997. Recovery of crenarchaeotal ribosomal DNA sequences from freshwater-lake sediments. Appl. Environ. Microbiol. 63, 321-323.
Schlitzer, R., 2001. Ocean Data View, http://www.awi-bremerhaven.de/GEO/ODV
Schouten, S., Hopmans, E.C., Schefuß, E., Sinninghe Damsté, J.S., 2002. Distributional variations in marine crenarchaeotal membrane lipids: a new tool for reconstructing ancient sea water temperatures? Earth Planet. Sc. Lett. 204, 265–274.
Schouten, S., Hopmans, E.C., Sinninghe Damsté, J.S., 2004. The effect of maturity and depositional redox conditions on archaeal tetraether lipid palaeothermometry. Org. Geochem. 35, 567-571.
Schouten, S., Huguet, C., Hopmans E.C., Kienhuis M.V.M., Sinninghe Damsté J.S., 2007. Analytical methodology for TEX86 paleothermometry by high-performance liquid chromatography/atmospheric pressure chemical ionization-mass spectrometry. Anal. Chem. 79, 2940-2944.
Schouten, S., Hopmans, E.C., van der Meer, J., Mets, A., Bard, E., Bianchi, T.S., Diefendorf, A., Escala, M., Freeman, K.H., Furukawa, Y., Huguet, C., Ingalls, A., Ménot-Combes, G., Nederbragt, A.J., Oba, M., Pearson, A., Pearson, E.J., Rosell-Melé, A., Schaeffer, P., Shah, S.R., Shanahan, T.M., Smith, R.W., Smittenberg, R., Talbot, H.M., Uchida, M., Van Mooy, B.A.S., Yamamoto, M., Zhang, Z.H., Sinninghe Damsté, J.S., 2009. An interlaboratory study of TEX86 and BIT analysis using high-performance liquid chromatography-mass spectrometry. G-Cubed 10, Q03012, doi:10.1029/2008GC002221.
Sinninghe Damsté, J.S., Hopmans, E.C., Schouten, S., van Duin, A.C.T., Geenevasen, J.A.J., 2002. Crenarchaeol: The characteristic glycerol dibiphytanyl glycerol tetraether membrane lipid of cosmopolitan pelagic Crenarchaeota. J. Lipid Res. 43, 1641–1651.
Sinninghe Damsté, J.S., Ossebaar, J., Abbas, B., Schouten, S., Verschuren, D., 2009. Fluxes and distribution of tetraether lipids in an equatorial African lake: Constraints on the application of the TEX_{86} palaeothermometer and BIT index in lacustrine settings. Geochim. Cosmochim. Ac. 73, 4232-4249.
Sinninghe Damsté, J.S., Rijpstra, W.I.C., Hopmans, E.C., Weijers, J.W.H., Foesel, B.U., Overmann, J., Dedysh, S.N., 2011. 13,16-Dimethyl octacosanedioic acid (iso-diabolic acid), a common membrane-spanning lipid of Acidobacteria subdivisions 1 and 3. Appl. Environ. Microbiol. 77, 4147-4154.
Sun, Q., Chu, G., Liu, M., Xie, M., Li, S., Ling, Y., Wang, X., Shi, L., Jia, G., Lü, H., 2011. Distributions and temperature dependence of branched glycerol dialkyl glycerol tetraethers in recent lacustrine sediments from China and Nepal. J. Geophys. Res. 116, G01008, doi:10.1029/2010JG001365.
Tierney, J.E., Russell, J.M., Eggermont, H., Hopmans, E.C., Verschuren, D., Sinninghe Damsté, J.S., 2010. Environmental controls on branched tetraether lipid distributions in tropical East African lake sediments. Geochim. Cosmochim. Ac. 74, 4902-4918.

559 Weijers, J.W.H., Schouten, S., Spaargaren, O., Sinninghe Damsté, J.S., 2006a.
560 Occurrence and distribution of tetraether membrane lipids in soils: Implications for
561 the use of the TEX_{86} proxy and the BIT index. Org. Geochem. 37, 1680-1693.
562 Weijers, J.W.H., Schouten, S., Hopmans, E.C., Geenevasen, J.A.J., David, O.R.P.,
563 Coleman, J.M., Pancost, R.D., Sinninghe Damsté, J.S., 2006b. Membrane lipids of
564 mesophilic anaerobic bacteria thriving in peats have typical archaeal traits. Environ.
565 Microbiol. 8, 648–657.
566 Weijers, J.W.H., Schouten, S., van den Donker, J.C., Hopmans, E.C., Sinninghe
567 Damsté, J.S., 2007. Environmental controls on bacterial tetraether membrane lipid
568 distribution in soils. Geochim. Cosmochim. Ac. 71, 703-713.
569 Weijers, J.W.H., Wiesenberg, G.L.B., Bol, R., Hopmans, E.C., Pancost, R.D., 2010.
570 Carbon isotopic composition of branched tetraether membrane lipids in soils suggest
571 a rapid turnover and a heterotrophic life style of their source organism(s).
572 Biogeosciences 7, 2959-2973.
573 Yamamoto, M., Okino, T., Sugisaki, S., Sakamoto, T., 2008. Late Pleistocene changes
574 in terrestrial biomarkers in sediments from the central Arctic Ocean. Org. Geochem.
575 39, 754-763.
576 Zink, K.-G., Vandergoes, M. J., Mangelsdorf, K., Dieffenbacher-Krall, A. C., Schwark,
577 L., 2010. Application of bacterial glycerol dialkyl glycerol tetraethers (GDGTs) to
578 develop modern and past temperature estimates from New Zealand lakes. Org.
579 Geochem. 41, 1060-1066.
580 Zhu, C., Weijers, J.W.H., Wagner, T., Pan, J.-M., Chen, J.-F., Pancost, R.D., 2011.
581 Sources and distributions of tetraetherlipids in surface sediments across a large river-
582 dominated continental margin. Org. Geochem. 42, 376-386.
583

584 # TABLES

585

586 **Table 1. Sites, Methods and Regression details:** Locations (numbers refer to map in
587 Figure 1) and methodologies (referring to numbers in the ´Material and Methods´
588 section) as well as references for previously published data sets. Regression details are
589 given for plots shown in Figures 2 and 3 for the correlation of brGDGTs (sum of *m/z*
590 1050, 1036, and 1022) vs. crenarchaeol. Statistics are given here as well for cyclized
591 brGDGTs vs. crenarchaeol (sum of *m/z* 1020, 1028, 1034, 1032, 1048, and 1046; not
592 shown in Figures). Cyclised brGDGTs were, however, not analysed for all sample sets
593 and "not determined" (nd) refers to sites where they were not. Brief site and data set
594 descriptions are shown in Appendix 1. Abbreviations: Ref. – References; Ext. –
595 extraction methods; Fract. – fractionation methods; Anal. – analytical methods.; n -
596 number of samples included; nd – not determined; ns – not significant. Coefficients of
597 determination and slopes are only given if statistically significant ($p<0.01$).

598
599

Data set	codes in Fig. 1	Methods			Latitude (°N)	Longitude (°E)	water depth (m)	Ref. for previously published GDGT data	n	Regression statistics			
		Ext.	Fract.	Anal.						major brGDGTs vs. Crenarchaeol		cycl. brGDGTs vs. Crenarchaeol	
										r^2	slope	r^2	slope
Lacustrine samples													
Lake Baikal:													
North - Holocene	L1	E1	F2	A1	54.0	108.9	386	Fietz et al. (2011b)	21	0.96	0.44	0.92	0.12
North - Last glacial	"	E1	F2	A1	"	"	"		60	0.80	0.46	0.83	0.18
North - Last interglacial	"	E1	F2	A1	"	"	"	Fietz et al. (2011a,b)	47	0.82	0.69	0.68	0.18
North - seasonal trap	L1	E1	F2	A1	54.5	109.1	920		6	0.94	0.42	ns	
North - annual trap	"	E1	F5	A2	"	"	"		6	0.97	0.13	0.92	<0.001
North - surface sediment	"	E1	F5	A2	"	"	"		10	0.98	0.15	ns	
South - Holocene	L2	E1	F5	A1	51.6	104.9	675		67	0.86	0.39	0.77	0.06
South - seasonal trap	L2	E1	F2	A1	51.7	105.0	1396		8	0.95	0.41	ns	
South - annual trap	"	E1	F5	A2	"	"	"		13	0.996	0.04	ns	
South - surface sediment	"	E1	F5	A2	"	"	"		10	0.99	0.51	0.97	<0.001
Centre - core	L3	E1	F5	A1	52.5	106.2	355		60	0.74	0.49	nd	
other lakes:													
Yamozero - core	L4	E1	F5	A2	65.0	50.1	3			ns		ns	
Bourget - core	L5	E1	F5	A2	45.8	5.8	106		22	0.95	0.41	0.94	0.15
Van - seasonal trap	L6	E1	F2	A1	38.6	42.8	440	Huguet et al. (2011)	8	0.81	4.08	nd	
Marine samples													
water column and surface sediment													
Chipana - POM	W1	E1	F6	A1	-21.3	-70.1	90			ns		nd	
North Sea - surface sediment	S1	E2	F2	A3	53 to 55	3 to 4.3	24 to 47	Herfort et al. (2006)	24	0.95[a]	0.10	nd	
Catalan Sea - surface sediment	S2	E1	F3	A1	39 to 41	-2 to -2.7	135 to 785		10	0.75	0.03	nd	
downcore sediment:													
Loch Sunart	C1	E3	F2, F3	A5	56.7	-5.9	50		39	0.74	0.53	nd	
Drammensfjord	C2	E2	F2	A3	59.7	10.4	100	Huguet et al. (2007b)	41	0.89	0.03	nd	
Skagerrak 2007	C3	E1	F5	A2	58.7	10.2	225		76	0.95	0.11	0.94	0.07
Skagerrak 2008	"	E1	F2	A1	"	"	"		28	0.85	0.20	0.90	0.16
Guaymas Basin	C4	E1	F5	A5	27.5	-112.1	881	McClymont et al. (in press)	146	0.81	0.02	nd	
Amazon Fan	C5	E4	F2	A4	5.8	-49.1	3346	Bendle et al. (2010)	43	0.65	0.91	0.60	0.10
Alaskan coast	C6	E1	F2	A1	55.6	-133.5	200		5	0.999	0.12	0.999	0.06
Fram Strait	C7	E1	F4	A1	78.9	6.8	1490	Fietz et al. (2011a)	43	0.57	0.07	0.57	0.07
NE Atlantic	C8	E1	F2	A1	51.8	-12.9	1153	Fietz et al. (2011a)		ns		ns	
equatorial Pacific	C9	E1	F1	A5	-1.6	-90.4	2580		30	0.79	0.01	nd	
subantarctic Atlantic	C10	E1	F1	A1	-42.9	9.0	3794	Fietz et al. (2011a,b)	127	0.89	0.06	0.82	0.05
Benguela current	C11	E1	F5	A1	13.0	-25.5	1992		50	0.74	0.02	0.89	0.01
equatorial Atlantic	C12	E1	F3	A1	3.0	-19.7	4849		10	0.84	0.61	0.94	0.20

[a] significant if one station, influenced by the English coastal current and turbidity plume, is omitted (Fig. 3K)

600 **Table 2. Correlation statistics for major branched GDGTs versus crenarchaeol as**
601 **related to total organic carbon (TOC; cf. Fig. 5) or to chlorophyll transformation**
602 **products (CHL):** Number of samples included (n), coefficients of determination (r^2)
603 and slopes. All correlations and slopes are significant with $p<0.001$, if not stated
604 otherwise. Details of the respective sample sets are given in Table 1. All data are
605 normalized. Normalization was accomplished by finding the sample with the highest
606 crenarchaeol/TOC concentration in a given sample set and then dividing all
607 crenarchaeol/TOC and brGDGTs/TOC data in that set by that value. The same
608 normalization was applied for the concentrations related to chlorophyll transformation
609 products. The GDGT, TOC and pigment concentration data were partly published
610 previously (Herfort et al., 2006; Huguet et al., 2007, 2011; Fietz et al., 2007, 2011;
611 Martínez-Garcia et al., 2009).

612

		major brGDGTs/TOC vs. crenarchaeol/TOC		**major brGDGTs/CHL. vs. crenarchaeol/CHL.**	
	ref. Fig. 1	**n**	**r^2**	**n**	**r^2**
Lake Baikal North Interglacial	L1	44	0.50	46	0.97
Lake Baikal Centre	L3	44	0.81	-	-
Baikal seasonal trap (North)	L1	-	-	6	0.99
Baikal seasonal trap (South)	L2	-	-	8	0.95
Lake Van seasonal trap	L6	8	0.50[a]	8	0.96
Drammensfjord	C2	41	0.81	-	-
Guaymas Basin	C4	-	-	144	0.84
Fram Strait	C7	-	-	43	0.77
subantarctic Atlantic	C10	-	-	126	0.40[b]
North Sea surface sediment compilation	S1	21	0.88	-	-

[a] $p=0.05$

613 [b] $r^2=0.94$ if only glacial periods are considered (n=69)

FIGURES

Figure 1. Map showing all sample locations; codes refer to Table 1. Map created using Ocean Data View (Schlitzer, 2001).

Figure 2. Correlations between crenarchaeol and branched GDGT concentrations per gram dry weight in lakes with significant ($p<0.01$) correlation. Lake Baikal (A) long-term records from North Basin (Fietz et al., 2011a,b), (B) long-term record from Buguldeyka uplift, (C) 10 cm upper surface sediment from South and North basins (Escala 2009), and (D) annual and monthly sediment traps from South and North basins; (E) Lake Bourget downcore record, and (F) Lake Van seasonal traps (Huguet et al., 2011). See Figure 1 for locations, Table 1 for site details and Appendix 1 for brief data set descriptions. Coefficients of determination (r^2) and slopes (x) are given for each data set. See also Table 1 for more regression details. All data are normalized and given here as relative units. Normalization was accomplished by finding the sample with the highest crenarchaeol value in a given sample set and then dividing all crenarchaeol and brGDGT data in that set by that value.

Figure 3. Correlations between crenarchaeol and branched GDGT concentrations per gram dry weight in marine sites with significant ($p<0.001$) correlation. (A-J) downcore records, (K-L) surface sediment sets (0-1cm). In the North Sea surface sediment compilation (K) the linear regression is given for samples influenced by the Dutch Coast and Channel waters (DCC) omitting the station Central Southern Bight (CSB) influenced by the English Channel and Turbidity plume (see Herfort et al., 2006). Some data sets were previously published (Herfort et al., 2006; Huguet et al., 2007; Bendle et al., 2010; Fietz et al, 2011a, 2011b). Coefficients of determination (r^2) and slopes (x) are given for each data set. See Figure 2 legend for site, regression and normalization details.

Figure 4. Sites without significant correlation between crenarchaeol and branched GDGT concentrations per gram dry weight ($p>0.01$). See Figure 2 legend for site and normalization details.

Figure 5. Correlations between crenarchaeol and branched GDGT normalized to total organic carbon (TOC) in (A) Lake Baikal North Basin Interglacial record, (B) Lake Baikal Buguldeyka uplift Holocene record, (C) Lake Van seasonal traps, (D) Drammensfjord record, and (E) North Sea surface sediment (0-1cm) compilation. In the North Sea surface sediment compilation (K) the linear regression is given for samples influenced by the Dutch Coast and Channel waters (DCC) omitting the station Central Southern Bight (CSB) influenced by the English Channel and Turbidity plume (see Herfort et al., 2006). Data were partly published previously (Herfort et al., 2006; Huguet et al., 2007, 2011; Fietz et al., 2011a, 2011b). See Figure 2 legend for site, regression and normalization details.

Figure 1

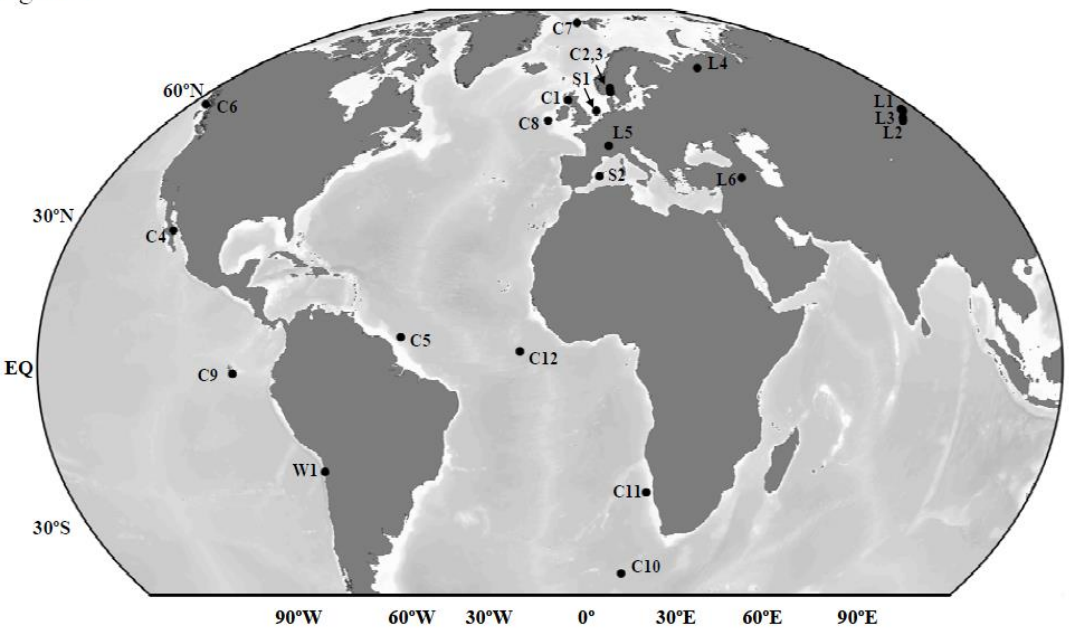

653

654

Figure 2

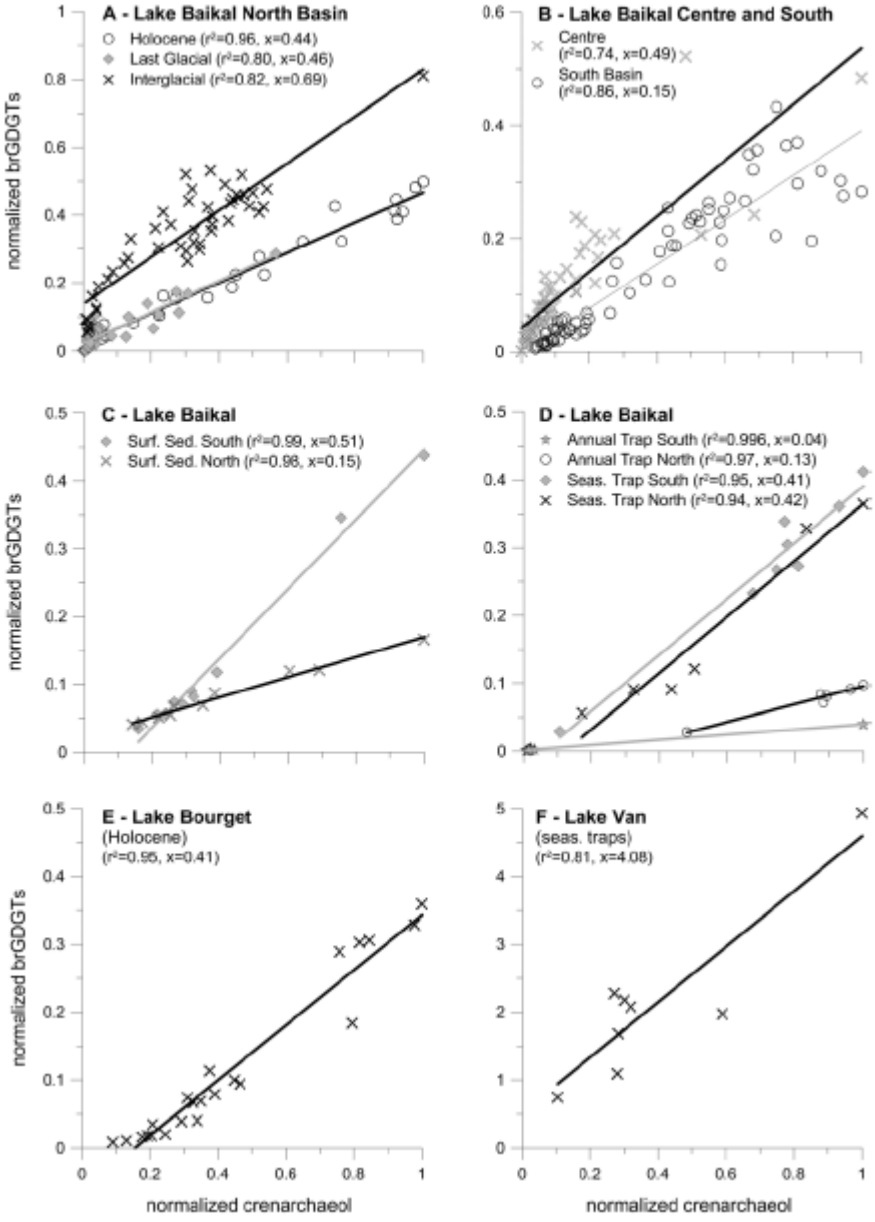

655

656

Figure 3

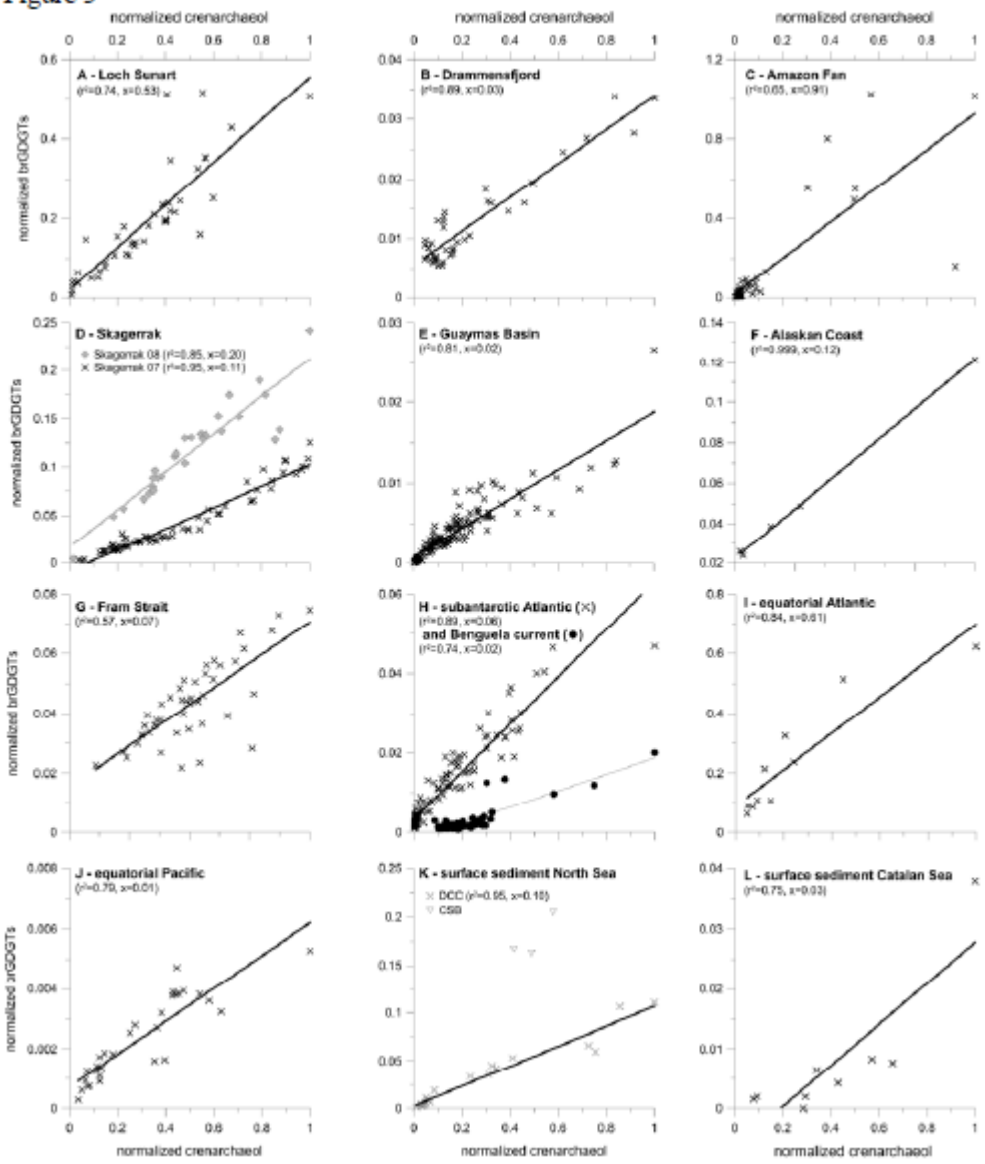

657

658

Figure 4

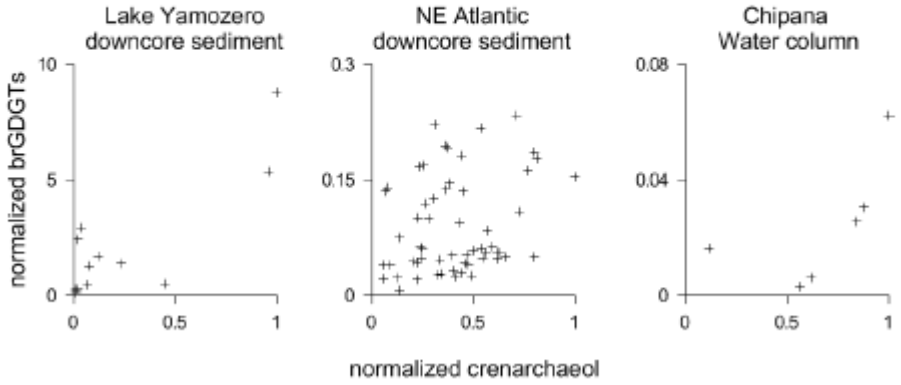

659

660

Figure 5

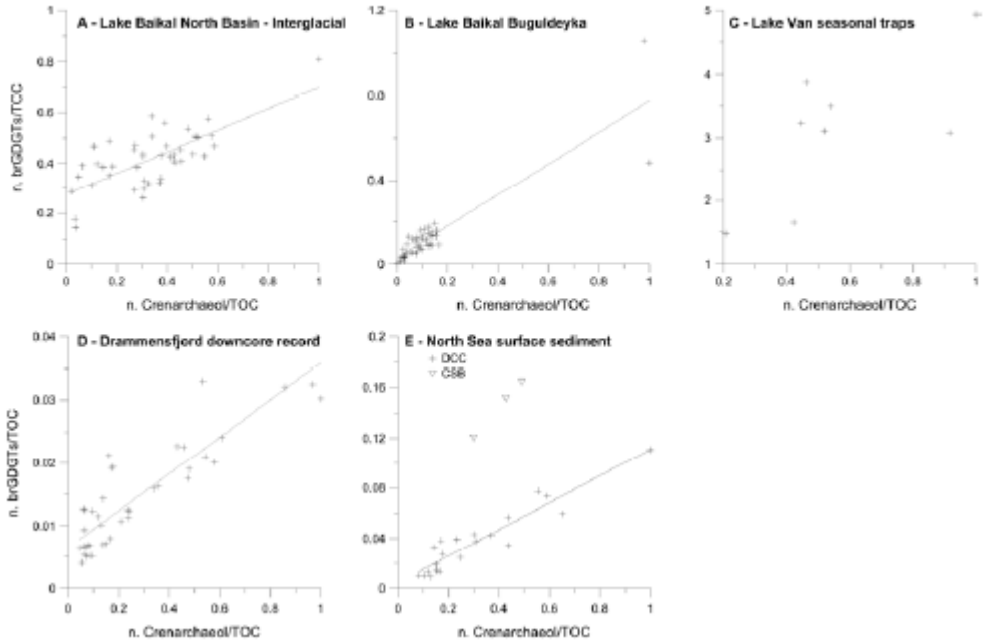

661

662

Appendix 1: Brief description of each sampling location and data set (e.g., geographic location, major environmental features, time span of data set for sediment cores or deployment of traps, and reference literature).

1. Lacustrine samples

Lake Baikal (central Siberia) is the World's deepest lake (ca. 1.6 km) and also one of the largest (ca. 600 km long). The water column remains oxygenated throughout the year. The lake is oligotrophic with periodic massive diatom blooms (Kozhov and Izmest'yeva, 1998). The Selenga River is the largest tributary into the central lake and has built up an enormous delta region. Lake Baikal downcore sediments were recovered from the North and South Basins (Oberhänsli and Mackay, 2005), and from the Buguldeyka Uplift in front of the Selenga Delta (Karabanov et al., 2008). The North Basin Last Interglacial record spans ca. 113-129 thousand years before present (ky BP; Fietz et al. 2007), the North Basin Last Glacial record spans ca. 12-57 ky BP, and the North Basin Holocene record the last 12 ky. The South Basin and Buguldeyka Uplift records also cover the Holocene but only part of the Last Glacial (<30 ky). Two surface sediment cores (upper 10 cm) were recovered in 2001 from the North and South basins. Both coring sites are located at a distance of ca. 400 km from each other. The North is ice covered for longer and has a shorter vegetation period than the South, and it has an overall lower sedimentation rate resulting in deeper oxic and oxygenized sediment depth (Müller et al., 2005). Annually integrating sediment traps were deployed in June 2001 at 6 different depths along the 920 m deep water column in the North, and at 14 different depths along the 1396 m deep water column in the South (Fietz et al. 2005). Seasonal traps were deployed on the same moorings than the annually integrating traps below the upper mixed water layers and above the lake bottom.

687 *Lake Yamozero*, located in northern Siberia outside the present zone of permafrost,
688 covers an area of c. 30 km^2, and has an almost circular outline with a maximum water
689 depth of ca. 3 m (Henriksen et al., 2008). The small catchment area of 95 km^2 consists
690 of mires near the shore and a boreal forest (Henriksen et al., 2008). A series of distinct
691 shorelines encircles the lake up to a level of about 15 m above the present lake level
692 (Henriksen et al., 2008). The downcore record from this lake spans ca. 1-22 m. *Lake*
693 *Bourget* is a mesotrophic lake located in front of the French Alps (42 km^2, 146 m deep,
694 Jacob et al., 2008). The catchment area is characterized by a local river watershed of
695 600 km^2 and sporadic major flooding events of the Rhône River (Jacob et al., 2007).
696 The record covers a time span of ca. 3.5-9 ky BP. *Lake Van* is situated in eastern
697 Anatolia (Turkey) and is the world's largest soda lake (3570 km^2, 460 m deep, pH ~9.5-
698 9.9 and ~21-24 ‰ salinity; cf. Stockhecke, 2008). It receives water mainly through
699 precipitation and snowmelt from a catchment area estimated to be 12500 km^2 (cf.
700 Stockhecke, 2008). Seasonal traps were deployed between June 2006 and August 2007
701 deep in the lake, just above the sediments (Stockhecke, 2008).

702 **2. Marine samples**

703 **2.1. Water column, sediment trap, and surface sediments samples**

704 *Chipana Bay* is located off Northern Chile in one of the most productive areas of the
705 Humboldt Current system, characterized by cold upwelling bottom waters. The nearest
706 river (Loa River) has almost no outflow except during El Niño events, when the
707 discharge increases due to intense precipitation. The data set includes filtered water
708 samples taken at three depths in both February and August 2007 at ca. 1 km off Chipana
709 Bay. The depths were: 1) fluorescence maximum, 2) upper boundary of the oxycline,
710 and 3) 1 m above the seabed (ca. 90 m). The *Catalan Sea*, in the North Western
711 Mediterranean (Spain), is a comparatively productive area in the mostly oligotrophic

712 Mediterranean. The data set includes surface sediment (0-1 cm) obtained from transects
713 between the city of Barcelona and the Balearic Islands, i.e., from the southward directed
714 Catalan coastal current to the northward flowing modified Atlantic waters. The southern
715 *North Sea* is a shallow shelf sea (<50 m) characterized by a predominant influence of
716 coastal runoff. The surface sediment samples (0-1 cm) were taken in February, April,
717 and August at seven stations located within or at the outflow of the Dutch coastal
718 waters, characterized by high riverine freshwater input, and channel water of recent
719 oceanic origin (see Herfort et al., 2006 for more details on sample collection). One
720 station was located in the English coastal waters and East Anglian turbidity plume
721 (Herfort et al., 2006).

722 **2.2. Downcore records**

723 *Loch Sunart* is a marine fjord located in northwest Scotland. The loch is approximately
724 31 km long with an average width of 1.5 km. Peat bogs occur in the catchment. The
725 record spans an interval of 145 to 1745 cm, which correspond to approximately 465-
726 6637 ky BP. *Drammensfjord* is located in southern Norway and is a hyposaline (salinity
727 <32) silled basin with a length of 20 km and a width of 1.6–3 km. The Drammen River
728 feeds the Drammensfjord introducing a large volume of particulate matter and creating a
729 brackish surface layer on top of the saline bottom waters (Huguet et al., 2007). The
730 downcore record spans the most recent period, approximately the past 70 y (Huguet et
731 al., 2007). The *Amazon Fan* is the third largest submarine delta and is situated off the
732 northeastern coast of Brazil. The major input pathway in the Amazon Fan is from the
733 outflow of the Amazon River with a wide backland catchment area (Bendle et al.,
734 2010). Biomarkers of unambiguous terrestrial origin dominate the sediments (Bendle et
735 al., 2010 and references therein). The record used here spans approximately 13 m,
736 which correspond to the last 20 ky (Bendle et al. 2010).

737 The *Skagerrak* is a strait located between the North and the Baltic Sea (Scandinavia).
738 The water circulation in the Skagerrak is counterclockwise, with Atlantic water entering
739 along the Danish coast and Baltic water outflowing along the Norwegian coast. Most
740 suspended sediments entering the Skagerrak are supplied by large volumes of Atlantic
741 water. The Glomma River is the largest river draining into the Skagerrak and enters the
742 sea close to the coring site (cf. Rueda et al., 2009). The data included in this study cover
743 approximately the past 2000 y (see Rueda et al., 2009 for past 200 ky). *Guaymas Basin*,
744 located in the central Gulf of California (Mexico), has high productivity and low-
745 oxygen bottom waters. It is influenced by North Pacific deep and intermediate water as
746 well as subequatorial subsurface and equatorial surface water. Nutrients are brought to
747 the surface by tidal mixing around the islands north of Guaymas Basin and wind-driven
748 upwelling, fuelling high phytoplankton productivity (Cheshire et al., 2005 and
749 references therein). The record used here spans the upper 38 m (McClymont et al., in
750 press).
751 The *Alaskan coast* site (Gulf of Esquibel, USA) is located in an area of coastal
752 downwelling which, however, supports relatively high marine productivity. The site is
753 in inland waters adjacent to heavily forested, steep terrains that are presently glaciated
754 only in upland regions (Walinsky et al., 2009). The Alaskan coast record here includes
755 five samples from five depth intervals of a gravity core (5, 50, 80, 120, 140 cm depth).
756 The *Fram Strait* is the passageway between Greenland and Svalbard through which
757 warm saline waters are transported northwards with the West Spitsbergen Current (the
758 end member of the North Atlantic Current) and fresh water and sea ice is exported
759 southwards with the East Greenland Current. This record was retrieved from the
760 western continental margin of Svalbard and spans the last ~2000 years (Spielhagen et
761 al., 2011). Most of the recent organic matter is autochthonous with terrestrial organic

matter supply being likely the result of long range sea-ice transport from the north, with contributions of the nearby Svalbard landmass (Birgel et al., 2004). The *NE Atlantic* site is located in the northwestern flank of the Porcupine Seabight. The site is situated close to a principal outlet glacier draining the British Ice Sheet and also receives ice rafted debris derived from other North Atlantic margins (Peck et al., 2006). The record comprises a sedimentary sequence with a time span of 15-25 ky, including two periods of massive ice rafted debris input (Heinrich events; cf. Peck et al., 2006).

The *equatorial Pacific* site is located east of Galapagos Islands and is influenced by the westwards flowing Southern Equatorial and the Peru Current Systems, including the Humboldt Current. Sediments in this region very likely contain particles from both windborne dust, transported by the southerlies, and submarine volcanic debris (Saukel et al., 2011). The coring site possibly contained some fluvial debris originating from the Gulf of Guayaquil on the eastern end of the Carnegie Ridge (Saukel et al., 2011). The record spans the upper 1.4 m. The *equatorial Atlantic* record is located in the open ocean within the southeastern margin of the Sierra Leone Rise. The region is characterized by excellent preservation of the calcareous organisms, high sedimentation rates, as well as windblown and fluvial delivery of diverse indicators of continental climate (Shipboard Scientific Party, 1988). The record comprises a time span of ca. 0.96 – 1.12 million y BP. The *Benguela current* site is located off the West African coast, where cold, nutrient-rich waters from the coastal upwelling area mix with low-productivity oceanic water and form a zone of intermediate productivity (Shipboard Scientific Party, 1998). The studied record covers approximately 340 m (ca. 2 million y BP). The *subantarctic Atlantic* site is located in the open ocean within the present day Subantarctic Zone (Martínez-Garcia et al., 2009, 2011). It is characterized by relatively low phytoplankton export production during interglacial periods and high export

production during glacial stages essentially stimulated by atmospheric supply of iron (Martínez-Garcia et al., 2009, 2011). The studied record covers a time span from the mid-Pleistocene to the Holocene, encompassing several glacial and interglacial cycles (MIS 1 to MIS 12, ca. 500 ky BP; Martínez-Garcia et al., 2009).

Appendix 1 References

Bendle, J.A., Weijers, J.W.H., Maslin, M.A., Sinninghe, Damsté J.S., Schouten, S., Hopmans, E.C., Boot, C.S. and Pancost, R.D., 2010. Major changes in glacial and Holocene terrestrial temperatures and sources of organic carbon recorded in the Amazon fan by tetraether lipids. Geochem. Geophys. Geosyst. 11, Q12007, doi:10.1029/2010GC003308

Birgel, D., Stein, R., Hefter, J., 2004. Aliphatic lipids in recent sediments of the Fram Strait/Yermak Plateau (Arctic Ocean): Composition, sources and transport processes. Mar. Chem. 88, 127-160.

Cheshire, H., Thurow, J., Nederbragt, A.J., 2005. Late Quaternary climate change record from two long sediment cores from Guaymas Basin, Gulf of California. J. Quaternary Sci. 20, 457–469.

Fietz, S., M. Sturm, Nicklisch A., 2005. Flux of lipophilic photosynthetic pigments to the surface sediments of Lake Baikal. Global Planet. Change 46, 29-44.

Fietz, S., Nicklisch, A., Oberhänsli, H., 2007. Phytoplankton response to climate changes in Lake Baikal during the Holocene and Kazantsevo Interglacials assessed from sedimentary pigments. J. Paleolimn. 37, 177-203.

Henriksen, M., Mangerud, J., Matiouchkov, A., Murray, A.S., Paus, A., Svendsen, J.I. 2008. Intriguing climatic shifts in a 90 kyr old lake record from northern Russia. Boreas 37, 20–37.

Herfort, L., Schouten, S., Boon, J.P., Wolering, M., Baas, M., Weijers, J.M.H., and Sinninghe Damsté, J.S., 2006. Characterization of transport and deposition of terrestrial organic matter in the southern North Sea using the BIT index. Limnol. Oceanogr. 51, 2196–2205.

Huguet, C., Smittenberg, R.H., Boer, W., Sinninghe Damsté, J.S., and Schouten, S. 2007. Twentieth century proxy records of temperature and soil organic matter input in the Drammensfjord, southern Norway. Org. Geochem. 38, 1838-1849.

Jacob, J., Disnar, J.-R., Arnaud, F., Chapron, E., Debret, M., Lallier-Vergès, E., Desmet, M., Revel-Rolland, M., 2008. Millet cultivation history in the French Alps as evidenced by a sedimentary molecule. J. Archaeol. Sci. 35, 814-820.

Karabanov, E.B., Prokopenko, A.A., Williams, D.F., Khursevich, G.K., 2000. A new record of Holocene climate change from the bottom sediments of Lake Baikal. Palaeogeogr. Palaeocl. 156, 211–224.

Kozhov, O.M., Izmest'eva, L.R., 1998. Lake Baikal, Evolution and Biodiversity. Backhuys Publishers, Leiden.

Martínez-Garcia, A., Rosell-Melé, A., Geibert, W., Gersonde, R., Masqué, P., Gaspari, V., Barbante, C., 2009. Links between iron supply, marine productivity, sea surface temperatures and CO_2 over the last 1.1My. Paleoceanography, PA1207. DOI: 10.1029/2008PA001657

Martínez-Garcia, A., Rosell-Melé, A., Jaccard, S.L., Geibert, W., Sigman, D.M., Haug, G.H., 2011. Southern Ocean dust-climate coupling during the past 4 million years. Nature. doi: 10.1038/nature10310.

McClymont E.L., Ganeshram R., Pichevin L.E., Talbot H.M., van Dongen B.E., Thunell R.C., Haywood A.M., Singarayer J.S., Valdes P.J., *in press*. Sea-surface temperature records of Termination 1 in the Gulf of California: challenges for seasonal and inter-annual analogues of tropical Pacific climate change (2011PA002226).

Müller, B., Maerki, M., Schmid, M., Vologina, E., Wehrli, B., Wüest, A., Sturm, M., 2005. Internal carbon and nutrient cycling in Lake Baikal: sedimentation, upwelling and early diagenesis. Global Planet. Change 46, 101-124.

Oberhänsli, H., Mackay, A.W., 2005. Introduction to 'Progress towards reconstructing past climate in Central Eurasia, with special emphasis on Lake Baikal'. Global Planet. Change 46, 1-7.

Peck, V. L., Hall, I., Zahn, R., Elderfield, H., Grousset, F., Hemming, S.R., Scourse, J.D., 2006. High resolution evidence for linkages between NW European ice sheet instability and Atlantic Meridional Overturning Circulation. Earth Planet. Sc. Lett. 243, 476-488.

Rueda, G., Rosell-Melé, A., Escala, M., Gyllencreutz, R., Backman, J., 2009. Comparison of instrumental and GDGT based estimates of sea surface and air temperatures from the Skagerrak. Org. Geochem. 40, 287-291.

Rueda, G., Fietz, S., Rosell-Melé, A., (subm.). Coupling of Air and Sea Temperatures in the Fram Strait during the Last 2000 Years. Geophys. Res. Lett.

Saukel, C., Lamy, F., Stuut, J.-B., Tiedemann, R., Vogt, C., 2011. Distribution and provenance of wind-blown SE Pacific surface sediments. Mar. Geol. 280, 130-142.

Shipboard Scientific Party, 1988. Introduction and explanatory notes. In: Ruddiman W., Sarnthein M., Baldauf J., et al. (Eds.) Proc. ODP, Init. Repts., 108: College Station, TX (Ocean Drilling Program). doi:10.2973/odp.proc.ir.108.101.1988

Shipboard Scientific Party, 1998. Site 1084. In: Wefer, G., Berger, W.H., Richter, C., et al., 1998. Proc. ODP, Init. Repts., 175: College Station, TX (Ocean Drilling Program). doi:10.2973/odp.proc.ir.175.1998

Spielhagen, R.F., Werner, K., Aagaard Sørensen, S., Zamelczyk, K., Kandiano, E., Budeus, G., Husum, K., Marchitto, T.M., Hald, M., 2011. Enhanced Modern Heat Transfer to the Arctic by Warm Atlantic Water. Science 331, 450-453.

Stockhecke, M., 2008. The annual particle cycle of Lake Van: Insights from space, sediments and water column. M.S. thesis. University of Zurich.

Walinsky, S.E., Prahl, F.G., Mix, A.C., Finney, B.P., 2009. Distribution and composition of organic matter in coastal southeast Alaskan surface sediments. Cont. Shelf Res. 29, 1565-1579.